

## Investigation on Electro Discharge Machining of H13

Nosratollah Solhjoei, Amir Vafaei, Forood Khalilzadeh and Keyvan Vafaei

Department of Mechanical Engineering, Najafabad Branch, Islamic Azad University, Najafabad, Isfahan, Iran

**Abstract:** Electrical Discharge Machining (EDM) is a well-established machining option for manufacturing geometrically complex or hard material parts that are extremely difficult-to-machine by conventional machining processes. The non-contact machining technique has been continuously evolving from a mere tool and die making process to a micro-scale application machining alternative attracting a significant amount of research interests. AISI H13 hot work steel is the tool material most commonly used in hot working processes. In this paper an attempt has been made to develop mathematical models for relating the Material Removal Rate (MRR) and Stability factor ( $S_p$ ) to input parameters (current, pulse-on time and voltage) in the EDM of H13. A Central Composite Design (CCD) involving three variables with three levels has been employed. Furthermore, a study was carried out to analyze the effects of machining parameters in respect of listed technological characteristics. The results of analysis of variance (ANOVA) indicate that the proposed mathematical models, can adequately describe the performance of the process within the range of the factors being studied. The experimental and predicted values were in a good agreement.

**Keywords:** AISI H13, electrical discharge machining (EDM), linear regression technique, material removal rate (MRR), response surface methodology

### INTRODUCTION

The origin of Electrical Discharge Machining (EDM) dates back to 1770 when an English scientist Joseph Priestly discovered the erosive effect of electrical discharges. The destructive effect of an electrical discharge was channelized and a controlled process for machining materials was developed (Ho and Newman, 2003). Electrical Discharge Machining (EDM) is known to be applicable to conductive material regardless of their physical and mechanical properties. EDM is used widely in machining hard metals and alloys in aerospace, automotive and die industries. In the EDM process the material is removed by successive electrical discharges occurring between an electrode and a work piece immersed in a dielectric fluid. Every discharge ionizes a very restricted area between, the closest opposing peaks of roughness of the electrodes and generates a localized plasma channel, within a vapor bubble bridge, in which the temperature can be as high as 8000-10000°C (Descoedres, 2005). The plasma pressure has been estimated to be up to several hundreds of bars. This hot plasma may lead to melting and evaporate of both electrodes (Das *et al.*, 2003). At the end of the pulse, when the current is stopped, the pressure suddenly falls,

causing the superheated molten liquid on the surface of both electrodes to explode into the liquid dielectric, leaving a crater on the electrode surfaces and creating small solid and/or hollow debris (Das *et al.*, 2003; Descoedres, 2005; Shabgard *et al.*, 2006).

Since EDM is a complex machining process, in order to achieve the economic objective of this process, optimal cutting conditions have to be determined and so mathematical models need to be established; Therefore, Statistical-mathematical models are always used by scientists to describe the correlation between characteristics and machining output results and setting or input parameters. The Fuzzy Theory, Artificial Neural Network and Regression Analysis are the most important and major modeling methods, employed in the EDM process modeling. Moreover, Regression analysis is regarded as a powerful tool for representing the correlation between input parameters and process responses in comparison with the other modeling methods (Jameson, 2001; Puertas *et al.*, 2004; Mukherjee and Ray, 2006; Fonda *et al.*, 2007).

Using regression analysis (Puertas *et al.*, 2005) presented mathematical models for electric discharge machining of WC-Co, SiC and conductive ceramics on the basis of experiment designing techniques. With regard

to electrode wear ratio, it has been confirmed that in all cases, the intensity factor was the most influential, followed by its own pure quadratic effect and the interaction effect of intensity and pulse time (Puertas *et al.*, 2005; Hewidy *et al.*, 2005; Mukherjee and Ray, 2006). Khoshkish *et al.* (2008) made a tremendous effort to analyze the effects of electrode tool materials and machining input parameters on AISI D3 EDM process characteristic, by the use of variance analysis and experiments designing techniques. It was pointed out that the graphite electrode, having highest material removal rate and precise dimension and low tool wear ratio, is the most appropriate material for Tool Steel machining. George used regression models and illustrated response surfaces for carbon-carbon composite and concluded that the most important input parameter, affecting the EDM process characteristic, is the peak current (George *et al.*, 2007).

In line with current knowledge, the main inconvenience when applying the EDM technology to the treatment of hardened dies is the low machining productivity. Otherwise, the selection of cutting parameters for obtaining higher cutting efficiency in EDM of dies which is made of H13 Tool Steel is still not fully solved; even with the most several studies were made on EDM of other materials in the open literature. This is mainly due to the nature of the complicated stochastic process mechanisms in EDM (Mukherjee and Ray, 2006). As a result, in the present study, the relationship between input parameters of EDM process, such as peak current, pulse-on time, voltage and the process outputs, namely MRR and  $S_f$  (Stability factor of process) have been modeled, using the techniques of Design of Experiments (DOE) method, multi linear regression techniques and Response Surface Methodology (RSM). Likewise the impacts of input parameters on the characteristics of machining of H13 Tool Steel have been analyzed. The results of this research lead to desirable process outputs (MRR and  $S_f$ ) and economical industrial machining, by optimum selection of the cited input parameters.

## MATERIALS AND METHODS

**Experimental apparatus:** Experiments were performed on a CNC Die-Sinking ED machine of type CHARMILLES ROBOFORM200 equipped with an Iso-pulse generator. The tool and work piece mass change were measured by using a digital balance (CP224S-Surtorius) with readability of 0.1 mgr. To control the process, monitoring of input parameters and recording of EDM pulses an electronic circuit was designed and made. This electronic circuit was employed to capture the gap voltage and current variations against time, which were then transferred and stored on a PC hard disk through a

serial cable and port connection. CSNE151-100 is utilized to monitor the current of the EDM process. Also the transformer is used to reduce and obtain both the positive and negative voltage amplitude. The diode bridge, capacitors and the regulators (LM7812C and LM7912C) are applied to achieve a regulated DC voltage as the power supply of the CSNE151 sensor. The primary winding of the sensor is wound around the electrode with one turn. The secondary has 1000 turns so the current amplitude is reduced by 0.001. The output of the sensor is a current in milliamperes. The resistor,  $R_m$  changes the output current into a measurable voltage so the waveform of the current can be monitored through the oscilloscope. The probe of the oscilloscope is connected to the tool and the workpiece directly, in order to measure the voltage amplitude between them.

**Materials:** The material used for workpiece was AISI H13 Tool Steel. The H13 samples were pre-heated in a 700°C salt bath, austenitized at 102°C in another salt bath, oil-quenched and repeatedly tempered at 560°C and cooled in air twice to produce the desired structure. The time of tempering was from 15 to 150 min. Blocks of hardened H13 were cut to circular tablets 20 mm height by wire EDM and then ground to parallel faces. EC-16 graphite tool electrode material has a particle size from 3 to 5 micron. Graphite tools were cut from 20 mm dia. Rod and machined by using a very accurate CNC lathe. Table 1 shows the workpiece and tool physical and mechanical properties.

**Design of experiments:** In the present section, the design factors and response variables selected for this work, as well as the methodology employed for the experimentation, will be described.

**Design factors selected:** There are a large number of factors to consider within the EDM process, but in this work peak current ( $I$ ), pulse-on time ( $T_{on}$ ) and voltage ( $V$ ) have only been taken into account as design factors. Regarding the point that the pulse energy per discharge depends on cited parameters considerably Eq. (1), in this research they opted as design factors:

$$w = \int_0^{T_{on}} V(t)I(t)dt \quad (1)$$

where  $W$  is the pulse energy per discharge ( $w$ ),  $V(t)$  is the pulse voltage ( $v$ ),  $I(t)$  is the pulse current ( $A$ ) and  $T_{on}$  is the pulse-on time ( $\mu s$ ).

**Response variables selected:** The response variables selected for this study refer to the speed of the EDM process, i.e., Material Removal Rate ( $MRR$ ) and the

Table 1: Work piece and tool Electrodes physical properties

Properties of H13 (workpiece)		Properties of EC-16 (graphite tool)	
Density	7.7252 ( $\times 1000 \text{ kg/m}^3$ )	Bulk density	1.811 ( $\text{g/cm}^3$ )
Melting point	2600 ( $^{\circ}\text{C}$ )	Specific resistance	1650 ( $\mu\text{ohm-cm}$ )
Poisson's ratio	0.30	Flexural strength	750 ( $\text{kg/cm}^2$ )
Elastic modulus	200 (Gpa)	Shore hardness	70
Hardness	52.7 HRC		
Thermal conductivity	28.6 (W/m.K)		

Table 2: Factors and levels selected for the experiments

Factors	Levels		
	-1	0	+1
Current (A)	8	12	16
Pulse-on time ( $\mu\text{s}$ )	12.8	25	50
Voltage (v)	120	160	200

Table 3: Experimental conditions and process variables

Condition and variables	Description
Generator type	Iso pulse H13 tool steel (20 mm diameter and 20 mm length)
Work piece	
Tool	Graphite EC-16 (18 mm diameter and 20 mm length)
Tool polarity	Positive
Dielectric	Oil flux ELF2
Flashing type	Normal submerged
Gap ( $\mu\text{m}$ )	0.09
Current (A)	8, 16, 24
Pulse-on time ( $\mu\text{s}$ )	12.8, 25, 50
Voltage (v)	120, 160, 200
Reference voltage (v)	70
Pulse-off time ( $\mu\text{s}$ )	6.4

Table 4: The matrix of order and design of the experiments and the test outputs

No. of EXE	Current (A)	Pulse-on time ( $\mu\text{s}$ )	Voltage (v)	MRR ( $\text{mm}^3/\text{min}$ )	$S_f$
1	-1	-1	-1	3.8377	0.231
2	+1	-1	-1	12.3854	0.072
3	-1	+1	-1	3.4019	0.301
4	+1	+1	-1	24.5197	0.114
5	-1	-1	+1	9.3262	0.397
6	+1	-1	+1	17.3411	0.143
7	-1	+1	+1	9.7004	0.513
8	+1	+1	+1	32.6304	0.222
9	0	0	0	18.9472	0.245
10	0	0	0	19.4196	0.235
11	0	0	0	18.6958	0.245
12	-1	0	0	8.9117	0.375
13	+1	0	0	22.9953	0.154
14	0	-1	0	14.5257	0.203
15	0	+1	0	20.7852	0.288
16	0	0	-1	13.7771	0.159
17	0	0	+1	21.2209	0.294

process stability factor that is named  $S_f$ .  $MRR$  is defined by the following equations:

$$MRR = \frac{VMR_p}{T} \quad (2)$$

where,  $MRR$  is the material removal rate ( $\text{mm}^3/\text{min}$ ),  $VMR_p$  is the difference of the sample volume in  $\text{mm}^3$ ,

before and after the machining process,  $VMR_E$  is the tool lost volume ( $\text{mm}^3$ ) during the machining process and  $T$  is the machining time (min).

The EDM process stability is determined by the proportion of abnormal discharges in the gap between a workpiece and an electrode, i.e. arc discharges and open-circuits, which not only lower the material removal rate, but also increase the tool wear.

The %NNP, %NOC and %NAD symbols were defined according to the following rules:

$$\%NNP = \frac{\text{Number of Normal Pulses}}{\text{Number of all pulses}} \times 100 \quad (3)$$

$$\%NOC = \frac{\text{Number of Open Circuits}}{\text{Number of all pulses}} \times 100 \quad (4)$$

$$\%NAD = \frac{\text{Number of Arc Discharges}}{\text{Number of all pulses}} \times 100 \quad (5)$$

Moreover, the  $S_f$  parameter which is represented the Stability factor of EDM machining process, is evaluated using Eq. (6):

$$S_f = (\%NNP) / (\%NOC + \%NAD + \%NNP) \quad (6)$$

where,  $S_f$  is the stability factor of process.

**Fractional factorial design employed:** Experiments were designed on the basis of the experimental design technique that has been proposed by Box and Hunter (Montgomery, 1997). The design which was finally chosen was a factorial design  $2^3$  with three central points, which provide protection against curvature and a total of 11 experiments were made. Consequently, for the case of the response variables which were not adequate for the previous first order model, this was widened by the addition of six star points, giving then a central composite design made up of the star points situated in the centers of the faces; that is to say, a total of 17 experiments in the case of this second order model. A summary of the levels selected for the factors to be studied is represented in Table 2. In addition, all the experimental conditions and variables considered in the tests are listed in Table 3.

Table 4 depicts the design matrix for the second-order models as well as the values obtained in the experiments for the response variables studied in this work, i.e.,  $MRR$  and  $S_f$ . As can be observed in this Table,

rows 1-8 correspond to the fractional factorial design, rows 9-11 correspond to the central points and finally, the star points are placed in the six last rows of the design matrix.

**RESPONSE SURFACES METHODOLOGY**

Response surface methodology approach is the procedure for determining the relationship between various process parameters with the various machining criteria and exploring the effect of these process parameters on the coupled responses (Mukherjee and Ray, 2006). In order to study the effect of EDM input parameters of H13 on MRR and  $S_f$  a second-order polynomial response can be fitted into the following equation:

$$Y = \beta_0 + \beta_1 X + \beta_2 \Phi + \beta_3 \Psi + \beta_{12} X\Phi + \beta_{13} X\Psi + \beta_{23} \Phi \Psi + \beta_{11} X^2 + \beta_{22} \Phi^2 + \beta_{33} \Psi^2 \quad (7)$$

where Y is the response and X, Φ, Ψ are the quantitative variables. β<sub>1</sub>, β<sub>2</sub> and β<sub>3</sub> represent the linear effect of X, Φ and Ψ respectively, β<sub>11</sub>, β<sub>22</sub> and β<sub>33</sub> represent the quadratic effects of X, Φ and Ψ. β<sub>12</sub>, β<sub>13</sub> and β<sub>23</sub> represent linear-by-linear interaction between “X and Φ”, “X and Ψ”, “Φ and Ψ” respectively. These quadratic models work quite well over the entire factor space and the regression coefficients were computed according to the least-squares procedure.

**EXPERIMENTAL RESULTS**

Table 4 illustrates the order, combination, design of the experiments and results of desired response surfaces (machining characteristics).

**Modeling response variables:** The Eq. (8), (9), (10) and (11) show the models for predictions and calculating MRR and S<sub>f</sub>:

$$\begin{aligned} \text{SQRT (MRR)} = & -8.51375 + 0.910681 + 0.01049T_{on} \\ & + 0.05737V - 0.02874I_c^2 - 0.0095T_{on}^2 - 0.0011V^2 \\ & + 0.00510IT_{on} - 0.00074IV + 0.000049T_{on} \cdot V \quad (8) \end{aligned}$$

$$\begin{aligned} \text{Exp}(S_f) = & 1.5891 - 0.01535I_c + 0.0042T_{on} - 0.0055V \\ & + 0.00065I_c^2 - 0.000071T_{on}^2 + 0.0000205V^2 \\ & + 0.0000513I_c \cdot T_{on} - 0.0000665I_c \cdot V + \\ & 0.0000064T_{on} \cdot V \quad (9) \end{aligned}$$

where, I<sub>c</sub> is the peak current (A), T<sub>on</sub> is the pulse-on time (μs) and V is the spark voltage (v). Table 5 and 6 show the variance analysis results of the introduced models. The P-value for each model in, mentioned Tables is less than 0.05, indicating that for a confidence level of 95%, the models are statistically significant and terms in the model have the significant effect on the responses.

Table 5: Variance analysis for the model of the MRR

Source	Sum of squares	d.f.	Mean squares	F-value	P-value
Model	17.173	9	1.908	284.7761	<0.0001
Residual	0.0475	7	0.0067		
Total	17.221	16			
R <sup>2</sup> Adjusted	0.9986				
R <sup>2</sup>	0.9972				
Standard error	0.0260				

Table 6: Variance analysis for the model of the S<sub>f</sub>

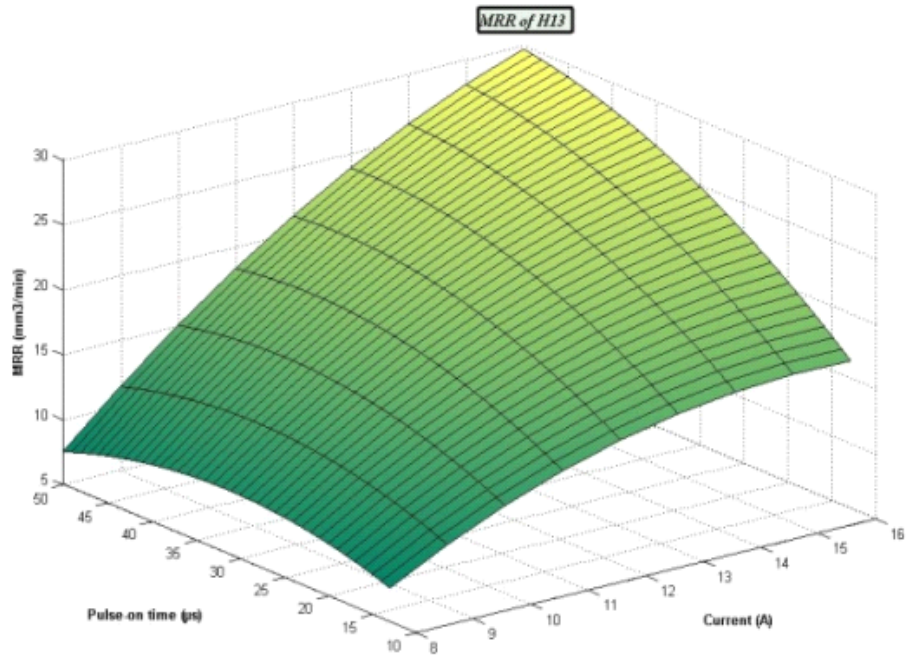
Source	Sum of squares	d.f.	Mean squares	F-value	P-value
Model	0.0289	9	0.0032	128.0921	<0.0001
Residual	0.0001	7	0.00003		
Total	0.0290	16			
R <sup>2</sup> AdjustedM	0.9939				
R <sup>2</sup>	0.9862				
Standard error	0.0050				

Table 7: Coefficient validation testing for the three responses

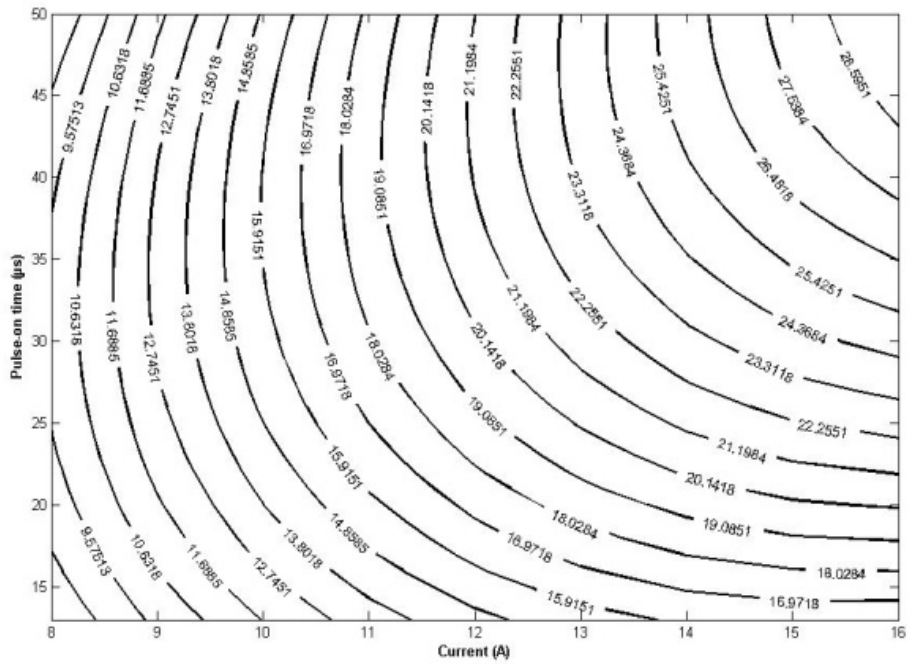
Predictor	Coefficients	T-test	P-value
<b>Response: SQRT (MRR)</b>			
Constant	-8.51375	-32.9168	<0.0001
Current (I <sub>c</sub> )	0.91068	35.1080	<0.0001
Pulse-on time (T <sub>on</sub> )	0.01049	2.4891	0.0416
Voltage(V)	0.05737	17.4646	<0.0001
Quad. I <sub>c</sub> (I <sub>c</sub> <sup>2</sup> )	- 0.02874	-28.8956	<0.0001
Quad. T <sub>on</sub> (T <sub>on</sub> <sup>2</sup> )	- 0.00095	-18.0303	<0.0001
Quad. V (V <sup>2</sup> )	- 0.00011	-12.0039	<0.0001
Interaction (I <sub>c</sub> T <sub>on</sub> )	0.005104	1.7421	<0.0001
Interaction (I <sub>c</sub> V)	0.00074	-13.0189	<0.0001
Interaction (T <sub>on</sub> V)	0.000049	4.0769	0.0047
<b>Response: Exp (S<sub>f</sub>)</b>			
Constant	0.8438	7.3766	0.0001
Current (I <sub>c</sub> )	-0.0320	-2.7917	0.0178
Pulse-on time (T <sub>on</sub> )	0.0047	2.5365	0.0011
Voltage (V)	0.0069	4.8092	0.00005
Quad. I <sub>c</sub> (I <sub>c</sub> <sup>2</sup> )	0.0018	4.21388	0.0107
Quad. T <sub>on</sub> (T <sub>on</sub> <sup>2</sup> )	-0.000050	-2.1624	0.0002
Quad. V (V <sup>2</sup> )	-0.0000076	-1.7376	0.00001
Interaction (I <sub>c</sub> T <sub>on</sub> )	-0.00026	-4.8394	0.0651
Interaction (I <sub>c</sub> V)	0.00025	-9.9951	0.0005
Interaction (T <sub>on</sub> V)	0.000026	4.9742	0.0291

Table 5 and 6 also demonstrate the values of R<sup>2</sup>-statistic and adjusted R<sup>2</sup>-statistic. The R<sup>2</sup> is defined as the ratio of variability explained by the model to the total variability in the actual data and is used as a measure of the goodness of fit. The more R<sup>2</sup> approaches unity, the better the model fits the experimental data. For instance, the obtained value of 0.996 for R<sup>2</sup> in the case of MRR (Table 5) implies that the model explains approximately 99.8% of the variability in MRR, whereas R<sup>2</sup> adjusted for the degrees of freedom is 0.997. Also the calculated values of R<sup>2</sup> in Table 5 and 6 confirm that the relationships between the independent factors and responses can adequately be explained by the models.

The adjusted R<sup>2</sup> is a modification of R<sup>2</sup> that adjusts for the number of explanatory terms in the model and the adjusted R<sup>2</sup> increases only if the new term improves the

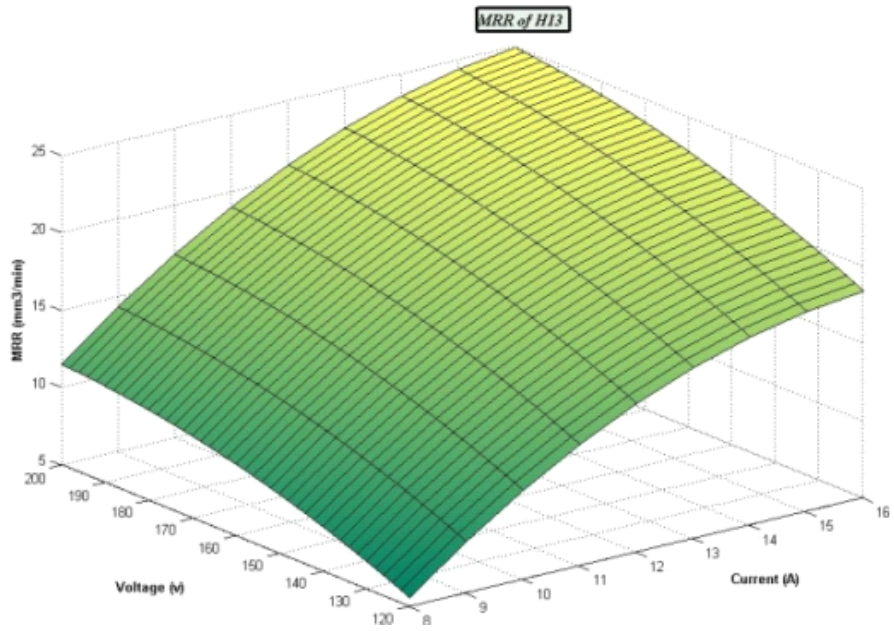


(a)

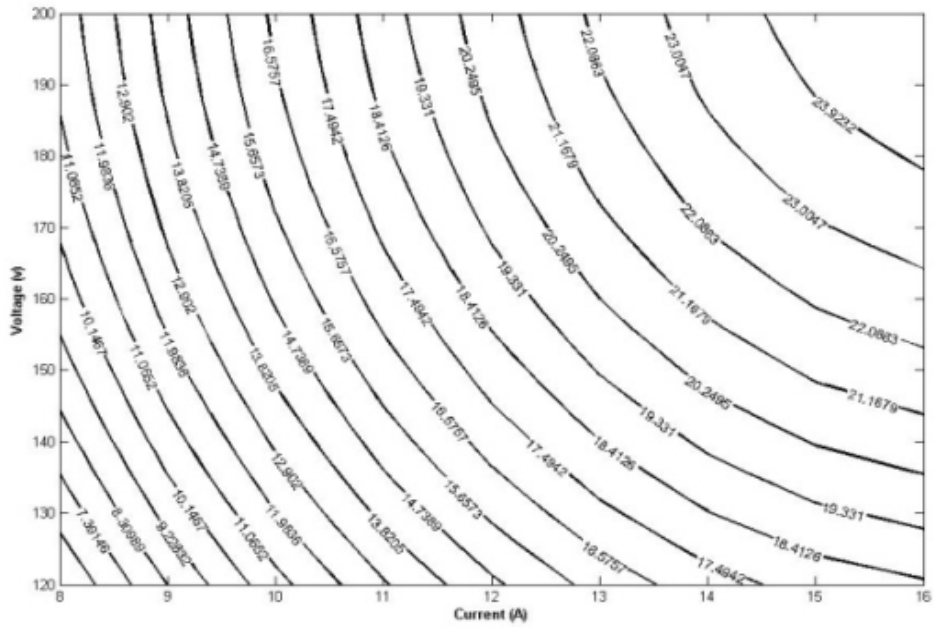


(b)

Fig. 1: a) Response surface, b) Contours of the material removal rate versus current and pulse-on time ( $V = 160$  v)

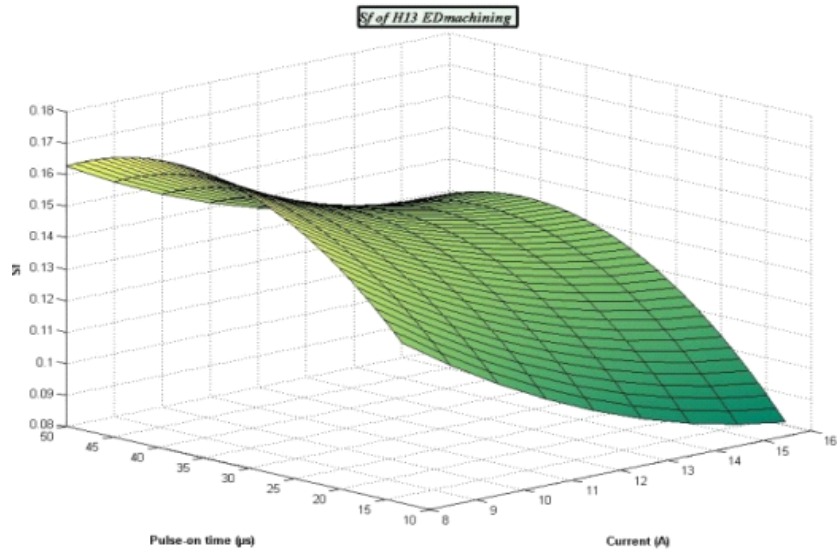


(a)

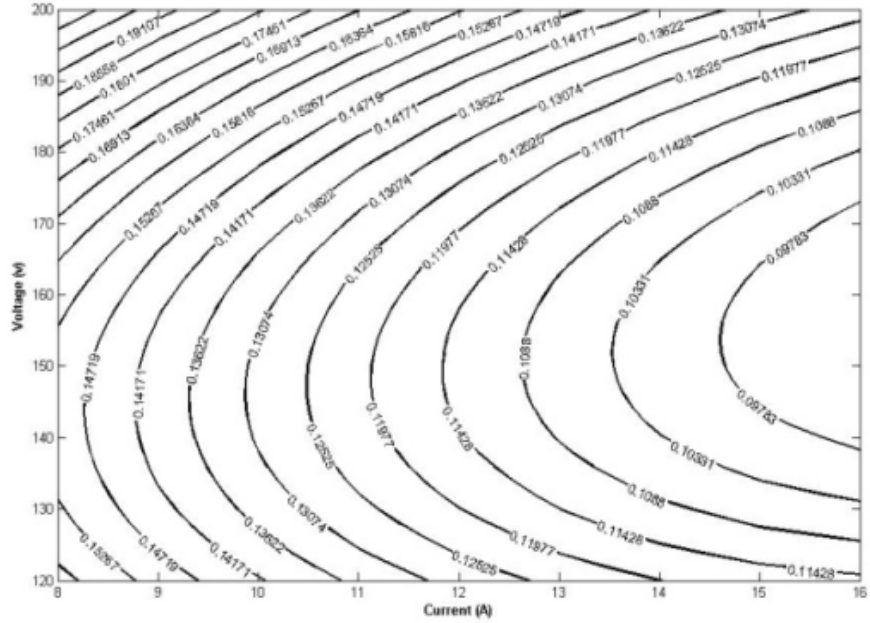


(b)

Fig. 2: a) Surface response, b) Contours of the material removal rate versus current and voltage ( $T_{on} = 25 \mu s$ )

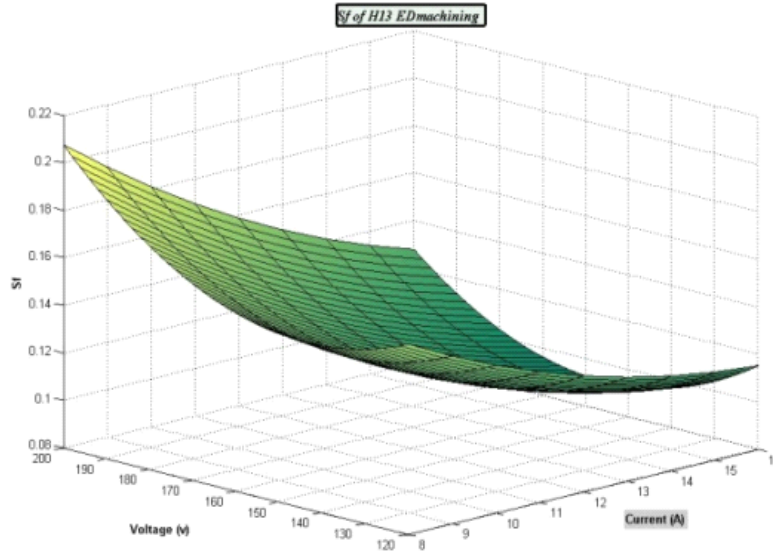


(a)

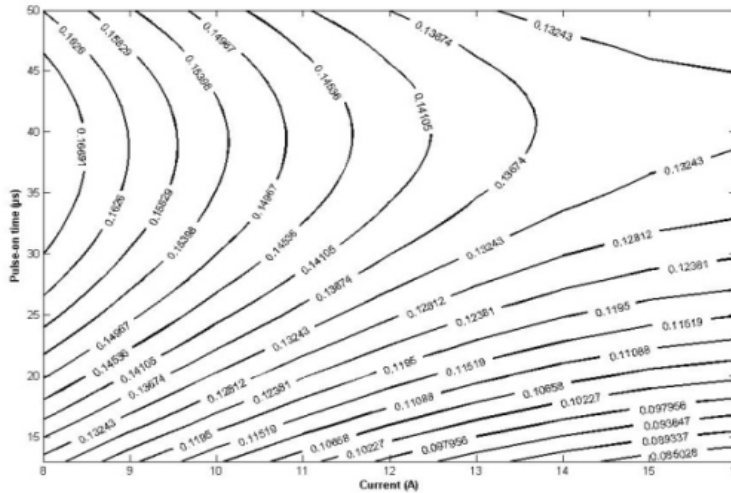


(b)

Fig. 3: a) Response surface, b) Contours of the stability factor versus current and pulse-on time (voltage = 160 v)



(a)



(b)

Fig. 4: a) Surface response, b) Contours of the stability factor versus current and voltage ( $T_{on} = 25 \mu s$ )

model more than would be expected by chance. Adjusted  $R^2$  does not have the same interpretation as  $R^2$  and it can be negative and will always be less than or equal to  $R^2$  (Montgomery, 1997).

Table 7 presents the values of  $\beta$  coefficients of models, in order to test the significance of each individual term in the models; a complete analysis of variance according to Student's t-test was performed. The calculated T-values as well as corresponding P-values are listed in Table 7 for the first response (SQRT (MRR)) that

results demonstrate a remarkable effect of all terms of the model, especially the ones related to the current. As can be observed, from the data in the Table 7, in the case of the Exp ( $S_p$ ) the coefficients for  $I_c \times T_{on}$  is negligible and therefore its effect is not significant for the cited model.

## DISCUSSION

**Effect of input parameters on MRR:** Material Removal Rate in EDM process is of crucial importance,

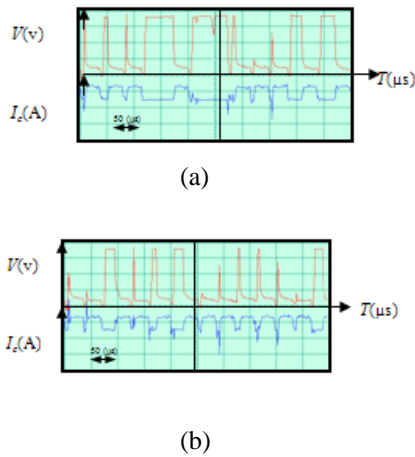


Fig. 5: Typical records of pulse shapes, a)  $T_{on} = 12.8 \mu s$ , b)  $T_{on} = 50 \mu s$  ( $I_c = 8A$ ,  $V = 200v$ )

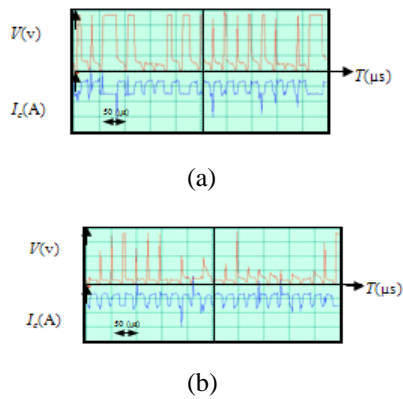


Fig. 6: Typical records of pulse shapes, a)  $T_{on} = 12.8 \mu s$ , b)  $T_{on} = 50 \mu s$  ( $I_c = 16A$ ,  $V = 200 v$ )

Figure 1 and 2 represent the response surfaces and contours of  $MRR$  versus current, pulse-on time and voltage.

The increase of current, pulse-on time and voltage values leads to an increase in the amount of Material Removal Rate. But the most substantial factors are peak current and pulse-on time. Additionally,  $MRR$  increase slightly with the voltage. The spark energy is a function of spark current, pulse-on time and voltage Eq. (1). Figure 1a and 2a indicate that an increase in discharge pulse duration time gives an initial significant increase in material removal rate and the further increase only leads to a very slight rise in material removal rate. The explanation for the  $MRR$  behavior after its maximum point is concerned to very high plasma diameter expansion due to the long discharge duration  $T_{on}$ , that diminishes pressure and energy of the plasma channel over the molten material of the electrodes. As a consequence, this phenomenon brings instability to the process lowering the material removal rate. Moreover,

high gap pollution and low energy density during high pulse-on time values lead the  $MRR$  to descend.

**Effects of input parameters on process stability and pulse shape:** Spark-erosion processes have often been analyzed and controlled by real time detection and evaluation of discharges in the gap. In this research during the experiments, information of pulse types was stored in PC. The detecting waveforms were plotted to elucidate the delay time and the abnormal electrical discharge, during EDM. Moreover, each appearing discharge is analyzed and pulse characteristics are compared with preset values.

Figure 3 and 4 show the predicted value of Stability factor ( $S_p$ ) of the process in terms of the current, pulse-on time and the voltage, generated by the regression model for the ED machining of H13 Tool Steel.

It is evident that, there is an overall trend to decrease of the stability of the process by altering the process mode to roughing regimes. Furthermore, these Figures reveal that the ratio of normal pulses to abnormal discharges ( $S_p$ ) in ED machining of H13 Tool Steel depends on the values of current, considerably. It is also noticeable from the same Figures that the pulse-on time and voltage has a limited effect on the  $S_p$  whereas the cited parameters caused a positive impact on the stability of the process. The results detailed above were confirmed by t-test data given in Table 7.

However, Fig. 5 and 6 depict the different discharging waveforms and the corresponding discharging effect for the different input parameters. It is obvious from Fig. 5 a that the occurrence of open-circuit pulses is the most considerable phenomenon in finishing modes. Gap conditions in EDM are random in nature in terms of dielectric condition and gap size. In finishing modes, the control of the process is difficult, because in these stages the gap between the electrodes becomes smaller. So the control system has to regulate a smaller gap. This makes the control task more complex and accumulated debris may build a bridge between the electrodes, allowing short-circuit to occur. Moreover, reactions of control system to occurrence of short-circuit pulses leads to the occurrence of open-circuit pulses.

In addition, it is clear that in higher values of input parameters Fig. 5b and 6a, the delay time ( $T_d$ ) of each pulse is plummeted and occurrence of normal pulses is increased, consequently. It is due to the increase of Material Removal Rate and debris aggregation because of the increase in pulse Energy, in higher setting values. However, additional debris into the kerosene may enlarge the gap. This is because the additional debris facilitates the bridging effect and minimizes the insulating strength of the dielectric fluid, thus a discharging channel is easily formed and the delay time and the gap voltage between the electrode and the workpiece are considerably decreased. It leads to decreasing of short-circuit and open-circuit pulses' occurrence.

By further increase of pulse-on time, it is noticed that much instability was brought into the working gap in either the form of arc discharge pulses, probably due to insufficient interval time  $T_d$  between to successive discharges to evacuate the coarse eroded material and simultaneously de-ionize the working gap. As a consequence the overconcentration of dielectric and electrodes byproducts negatively interfered on the occurrence of normal discharges. Collection of debris in sparking gap, impurity, different compounds of hydrocarbons that are decomposed from hydrocarbonaceous dielectric and presence of decomposed gases (such as carbon monoxide, methane, etc.) prepare an especial condition that increase the arc pulses' occurrence and reduces machining efficiency. Therefore, it should be noted that when  $I_c$ ,  $T_{on}$  or  $V$  are increased the  $MRR$  parameter also tends to increase at least up to a maximum value (peak point), after which it tends to decrease due to that the increase of abnormal discharges overcome the rising of pulse energy.

Another remark to be made, deals with the strong correlation between Surface Roughness and the occurrence of arc pulses which have a close relatively with "level of contamination". When the level of contamination rises, concentration of contamination around the discharging point causes a level of electrical Conductivity that lead to an arc pulse, eventually. If occurrence of arc pulses will pursue, a pillar of carbon is made on surface of work piece. Penetration of this pillar of carbon into workpiece and tool surfaces causes reduction of surface quality. In addition, occurrence of an arc pulse causes a dramatic increase in maximum surface roughness ( $R_{max}$ ) and surface mean roughness, consequently.

## CONCLUSION

In this research, an experimental investigation was performed to consider the machining characteristics in EDM process of H13 Tool Steel and the following results were concluded:

- It has been confirmed that the regression technique can be successfully applied to model the input and output variable of electro discharge of H13 Tool Steel.
- The  $MRR$  value first increases with the increase of pulse-on time, but for the values further than a specific  $T_{on}$ , it starts to decrease, affected by some thermodynamic factors, independent of the current value.
- It is obvious that in lower values of pulse-on time and pulse current, the occurrence of open-circuit pulses is the most considerable phenomenon. But In higher values of pulse current (roughing modes), the level of arc pulses extremely increases.

- In spite of the increase in level of contamination and abnormal discharges, the rise of each pulse's energy in roughing modes resulted as increase in Material Removal Rate until peak points of  $MRR$  in each current's set.

## REFERENCES

- Ho, K.H., S.T. Newman, 2003. State of the art Electrical Discharge Machining (EDM). Int. J. Machine Tools Manufact., 43: 1287-1300.
- Descocudres, A., 2005. Characterization of electrical discharge machining plasmas. Ph.D. Thesis, Lausanne, EPFL.
- Das, S., M. Klotz, F. Klocke, 2003. EDM simulation: Finite element-based calculation of deformation, microstructure and residual stresses. J. Materials Process. Technol., 14: 434-451.
- Shabgard, M.R., A. Ivanov and A. Rees, 2006. Influence of EDM machining on surface integrity of WC-Co. Proceedings of the Second International Conference of Multi-Material Micro Manufacture (4M), France., pp:
- Jameson, E.C., 2001. Electrical Discharge Machining. Society of Manufacturing Engineering SME Publication, USA
- Khoshkish, Ashtiani and Goreyshi 2008. Effects of Tool electrode material on electrical discharging machining process of hardened tool AISI D3, Iran Conference of Manufacturing Engineering.
- Puertas, I., C.J. Luis and A. Álvarez, 2004, Analysis of the influence of EDM parameters on surface quality,  $MRR$  and  $EW$  of WC-Co. J. Mater. Process. Technol., 153-154: 1026-1032.
- Fonda, P., Z. Wang, K. Yamazaki and Y. Akutsu, 2007. A fundamental study on Ti-6Al-4V's thermal and electrical properties and their relation to EDM productivity, J. Mater. Process. Technol., 202 (1-3): 583-589.
- Mukherjee, I. and P.K. Ray, 2006. A review of optimization technique in metal cutting process. Comput. Indust. Eng., 50: 15-34.
- Hewidy, M.S., T.A. El-Taweel and M.F. El-Safty, 2005. Modelling the machining parameters of wire electrical discharge machining of Inconel 601 using RSM. J. Mater. Process. Technol., 169: 328-336.
- Puertas, I., C.J. Luis and G. Villa, 2005, Spacing roughness parameters study on the EDM of silicon carbide. J. Mater. Process. Technol., 164-165: 1590-1596.
- George, P.M., B.K. Raghunath, L.M. Manocha and A.M. Warriar, 2007, EDM machining of carbon-carbon composite-a Taguchi approach. J. Mater. Process. Technol., 153-154: 920-924.
- Montgomery, D.C., 1997, Design and Analysis of Experiments. Wiley, NewYork.